Cell and Tissue Research (2019) 376:341–351
https://doi.org/10.1007/s00441-019-03001-1

REGULAR ARTICLE

Intravitreal Ets1 siRNA alleviates choroidal neovascularization in a mouse model of age-related macular degeneration

Manhui Zhu[1] · Li Jiang[2] · You Yuan[1] · Lili Chen[1] · Xiaojuan Liu[3] · Juan Liang[1] · Qiujian Zhu[1] · Dongmei Ding[2] · E. Song[1]

Received: 6 October 2018 / Accepted: 29 January 2019 / Published online: 1 March 2019

Abstract

Choroidal neovascularization (CNV) is the basic feature of neovascular age-related macular degeneration (AMD), the leading cause of blindness in elders. Macrophages and microglia promote CNV via producing pro-angiogenic factors and inflammatory cytokines. Transcription factor E26 transformation specific-1 (Ets1) plays a pro-angiogenic role via its pro-inflammatory function. In this study, Ets1 increased and localized in the macrophages and microglia of a mouse laser-induced CNV region. Ets1 siRNA intravitreal injection ameliorated the leakage and area of CNV, as well as inhibiting the dysfunction of retinal pigment epithelium (RPE) cells and the activation of macrophages/microglia. Taken together, we provide a new insight into the molecular mechanism of CNV progression, in which Ets1 can be a new therapeutic target.

Keywords Choroidal neovascularization · Ets1 · Macrophages · Microglia · Activation

Introduction

Choroidal neovascularization (CNV) is the fundamental characteristic of neovascular age-related macular degeneration (AMD), which is the leading cause of blindness in industrial societies (Luu and Palczewski 2018). Vascular endothelial growth factor (VEGF) has been confirmed as the major influencing factor in CNV formation (D'Amore 1994). Following this discovery, the era of intravitreal anti-VEGF drugs emerged and is still the first-line therapy for CNV (Heier et al. 2012; Hussain and Ciulla 2017). Nevertheless, CNV reduction requires consecutive injections and results in a lifelong treatment for the vast majority of patients. Additionally, following 7 years of CNV onset, approximately 80% CNV patients have no response to anti-VEGF therapy (Bakri et al. 2018; Rofagha et al. 2013). Therefore, novel and fundamental approaches are necessary to investigate more effective therapeutic strategies associated with further cellular and molecular mechanisms.

Retinal pigment epithelium (RPE) cells, forming a single cell layer that separates blood vessels from photoreceptors, accomplish a critical role in retinal homoeostasis (Strauss 2005) and morbidity, such as neovascular AMD (Kaarniranta et al. 2013). RPE cells secret pro-inflammatory cytokines (Tseng et al. 2013), oxidative lipids (Mettu et al. 2012) and pro-angiogenesis molecules (Ford et al. 2011; Grossniklaus et al. 2002), promoting the neovascular AMD development. Additionally, a number of AMD-associated insults may disrupt RPE lysosomes. For example, the component of lipofuscin granules (LGs)-A2E has been shown to permeabilize RPE lysosomes, leading to progressive RPE cell dysfunction and death, often associated with drusen deposition (Schutt et al. 2002).

Recent studies have focused on the influence of mononuclear phagocytes, such as macrophages and microglia, on CNV. Macrophages and microglia promote neovascularization via producing pro-angiogenic factors, such as platelet-derived growth factor β (PDGF-β), fibroblast growth factor

Manhui Zhu, Li Jiang, Dongmei Ding and E. Song contributed equally to this work.

✉ Dongmei Ding
dingdm2005@aliyun.com

✉ E. Song
songe@suda.edu.cn

[1] Department of Ophthalmology, Lixiang Eye Hospital of Soochow University, Suzhou, Jiangsu, China

[2] Department of Ophthalmology, Laizhou City People's Hospital, Yantai, Shandong, China

[3] Department of Pathogen Biology, Medical College, Nantong University, Nantong, Jiangsu, China

1 (FGF-1), FGF-2 and transforming growth factor β1 (TGF-β1) in the laser spot and secreting inflammatory cytokines including tumor necrosis factor α (TNF-α), interleukin 6 (IL-6) and C-X-C motif chemokine ligand 1 (CXCL1) (Li et al. 2017). Systemic interferon β (IFN-β) therapy of a mouse laser-induced CNV model effectively attenuates microgliosis and macrophage responses in the early stage of disease and significantly reduces CNV size in the late phase (Luckoff et al. 2016). Additionally, direct inhibition of retinal microglia by minocycline dramatically suppresses CNV formation, which is associated with the migration inhibition of lectin positive cells, which are possibly retinal macrophages/microglia (Huang et al. 2013).

E26 transformation specific-1 (Ets1), the vital member of the E26 transformation-specific sequence (Ets) transcription factor family, is a master regulator of endothelial cell (EC) gene transcription. Upregulation of Ets1 in quiescent ECs is sufficient to convert them to an angiogenic state and the depletion of Ets1 impairs vascular development during embryogenesis (Oda et al. 1999; Wei et al. 2009). The Ets motif is found in nearly all angiogenic transcriptional enhancers (Hashiya et al. 2004). Ets1 also plays a pro-inflammatory role. For example, Ets1 mediates the formation of arterial neointima in a rat carotid artery balloon injury model by regulating the activation of pro-inflammatory cytokines and adhesion molecules, including IL-6, monocyte chemoattractant protein 1 (MCP-1), P-selectin and E-selectin (Feng et al. 2010). Additionally, Ets1 blockade results in significant reductions in glomerular injury score, fibronectin expression, proteinuria and macrophage infiltration in hypertensive Dahl salt-sensitive rats (Feng et al. 2015). However, the potential role and mechanism of Ets1 in CNV is unclear.

In the present study, Ets1 expression increased in a mouse laser-induced CNV model and localized in the macrophages and microglia of the CNV region. Ets1 siRNA intravitreal injection alleviated the leakage and area of CNV, as well as the dysfunction of RPE cells and the activation of macrophages/microglia inside the CNV region.

Materials and methods

Mouse laser-induced CNV model

Adult C57BL/6 (B6) mice (Experimental Animal Center of Soochow University, Suzhou, Jiangsu, China) were used for the CNV model construction. All animal experiments were performed in accordance with the requirements of the Animal Welfare Committee of Soochow University. The study adhered to the ARVO Statement for the Use of Animals in Ophthalmic and Vision Research. Adult C57BL/6J (B6) mice were anesthetized by intraperitoneal injection with 0.5% pentobarbital (0.1 ml per 10 g weight) and pupils were dilated with topical administration of tropic amide phenylephrine eye drops (Santen, Osaka, Japan). Laser photocoagulation (659 nm, 50-μm spot size, 0.05-s duration, 250 mW) with a hand-held contact fundus lens (Ocular Instruments, Bellevue, WA) was performed to burn the retina at the 3, 6, 9 and 12 o'clock positions. The time at which a bubble was observed, indicating rupture of Bruch's membrane, was recorded. All mice were randomly divided into six groups based on the time after laser treatment (normal, 1 day, 3 days, 7 days, 14 days and 28 days). For western blot analysis, each group contained 24 mice that received laser treatment and 15 mice that did not receive laser treatment constituted the normal group. In the normal and CNV 7-day groups, another 30 mice (60 eyeballs) were included for immunofluorescence and choroidal flat mount.

Western blot

To detect the protein level of molecules, we extracted mouse choroid-RPE-retina complex from three mice in the normal group and at 1 day, 3 days, 7 days, 14 days and 28 days after laser injury. Proteins and a molecular weight marker were separated by 10% SDS-PAGE and transferred to a PVDF membrane. The membrane was then incubated with primary antibodies for Ets1 (1:500; Abcam, Cambridge, MA, USA), VEGF (1:500; Santa Cruz Biotechnology) and GAPDH (1:2000; Santa Cruz Biotechnology). The antibodies were incubated in 5% skim milk overnight at 4 °C and reacted with HRP-conjugated secondary antibodies (1:2000; Thermo Scientific, Rockford, IL) at 37 °C for 2 h. The blots were then incubated with chemifluorescent reagent ECL (Thermo Scientific, Rockford, IL, USA) and exposed to X-ray film in the dark. The intensity of the GAPDH signal was used as an endogenous control and the band optical density was quantified by ImageJ software (National Institutes of Health, Bethesda, MD, USA).

Immunofluorescence

Ets1 tissue localization was examined on the 8-μm cryosections of eight eyes enucleated in each group (normal and day 7 after laser photocoagulation). The cryosections were blocked with 3% BSA for 4 h at room temperature, then incubated with Ets1, CD31, or F4/80 antibodies (all antibodies 1:50; Abcam, Cambridge, MA, USA) at 4 °C overnight. For CD31 staining, antigen retrieval was obtained via a heated water bath at 37 °C for 10 min. Thereafter, the slides were stained with Alexa Fluor 488 conjugated goat anti-mouse IgG, Alexa Fluor 546 conjugated goat anti-rabbit IgG (both antibodies 1:200; Invitrogen, Carlsbad, CA, USA) and DAPI (1:1000; Sigma-Aldrich). The photomicrographs were taken by a Leica TCS SP8 confocal microscope (Buffalo Grove, IL,

USA). Fluorescence and co-localization were analyzed using ImageJ software.

Intravitreal injection

The intravitreal injection of 1 μl of scramble siRNA, Ets1 siRNA (both siRNA 35 ng/μl; GenePharma, Suzhou, China), or vehicle (PBS solution) was given on day 3 and mice were killed on day 7 after laser treatment. The CNV 7-day group represented laser-induced CNV without any injection.

Fundus fluorescein angiography/indocyanine green angiography

To confirm the effect of Ets1 siRNA on CNV formation, fluorescein angiography was performed in the normal group or 7 days after laser photocoagulation. The development of CNV was evaluated using Heidelberg Spectralis HRA (Heidelberg, Germany) and images were captured 2 min after 0.3 ml of 2% fluorescein sodium (Alcon Laboratories, Fort Worth, TX, USA) or indocyanine green (ICG) (6 mg/kg; Sigma-Aldrich) was intraperitoneally injected.

Fundus autofluorescence

Fundus autofluorescence (FAF) was performed using the Heidelberg Spectralis HRA (Heidelberg, Germany). The pupils were dilated with topical tropicamide (0.5%; Alcon) and the cornea was lubricated with GenTeal Gel (Novartis) before examination. The outlines of the CNV lesions in FAF images were manually selected and the area and intensity of autofluorescence were analyzed by ImageJ software.

Choroidal flat mount and immunofluorescence staining

Eighteen eyes (six eyes from three mice/each group) of the normal, 7 days after laser treatment and Ets1-treated laser groups were used for choroidal flat mount and immunofluorescence staining. The eyes were enucleated and immediately fixed in 4% paraformaldehyde (Guoyao Group of Chemical Reagents, Beijing, China) in pH 7.3 PBS for 1 h. Under a biopsy microscope, the anterior segments were wiped out and the neurosensory retinas were detached and separated from the optic nerve head. The remaining eyecups were washed with cold ICC buffer (PBS containing 0.5% BSA, 0.2% Tween-20 and 0.1% Triton X-100). A 1 mg/ml solution of Alexa Fluor 488 conjugated Ets1 and Alexa Fluor 568 conjugated F4/80, Alexa Fluor 488 conjugated Ets1 and Alexa Fluor 568 conjugated Iba1, Alexa Fluor 568 conjugated phalloidin and Alexa Fluor 488 conjugated isolectin-B4 (IB4; 1:200; *Griffonia simplicifolia*), Alexa Fluor 488 conjugated IB4 and Alexa Fluor 568 conjugated CD68 were prepared in ICC buffer. All the antibodies are from Invitrogen-Molecular Probes (Carlsbad, CA, USA). The eyecups were incubated with the above fluorescent dyes in a humidified chamber at 4 °C with gentle shaking for 4 h, followed by washing with cold ICC buffer. Four or five radial cuts were made toward the optic nerve head for flat mounting of the sclera/choroid/RPE complexes with the gel (Gel-mount; Biomedia Corp., Foster City, CA). The samples were covered and sealed for confocal microscopic analysis. Iba1-positive cells were counted on stained choroidal flatmounts up to the ciliary body and on the outer segment side of the retina with ImageJ software (surface covered by fluorescein staining).

CNV volume quantification

Z-stack images of CNV retinal flat mounts stained with isolectin B4 were acquired using a laser scanning confocal microscope with a 10× objective lens. The image stacks were rendered in 3D using IMARIS imaging software (Carl Zeiss) and processed to digitally extract the fluorescent lesion area.

Statistical analysis

All data were represented as mean ± standard error of the mean (SEM). Comparisons were made by one-way ANOVA followed by Dunnet's *t* test. Statistical analysis was performed by using SPSS 13.0. $P < 0.05$ indicated statistical significance.

Results

Ets1 increases and localizes in the CNV region

To detect Ets1 expression following CNV, a mouse CNV model was constructed by laser photocoagulation. The Ets1 and VEGF protein level increased in the CNV group from 3 days, reaching a peak at 7 days, then declined to normal level at 28 days (Fig. 1a, b). Ets1 was co-localized with CD31 (a vascular endothelial marker) (Fig. 1d"'), indicating that Ets1 was localized in the CNV region. Additionally, Ets1 was co-localized with F4/80 (a macrophage/microglia marker; Fig. 1e") and Iba1 (also a macrophage/microglia marker; Fig. 1f"). In the normal group, there were no Iba1-positive cells in the choroid while Iba1-positive cells increased following CNV (Fig. 1g). The results suggest that Ets1 increases and localizes in the macrophages and microglia of the CNV region, giving a hint that Ets1 might participate in the pathogenesis of CNV.

Ets1 siRNA ameliorates the leakage of CNV

To confirm the role of Ets1 in CNV, Ets1 siRNA intravitreal (IVT) injection was applied in the mouse CNV model.

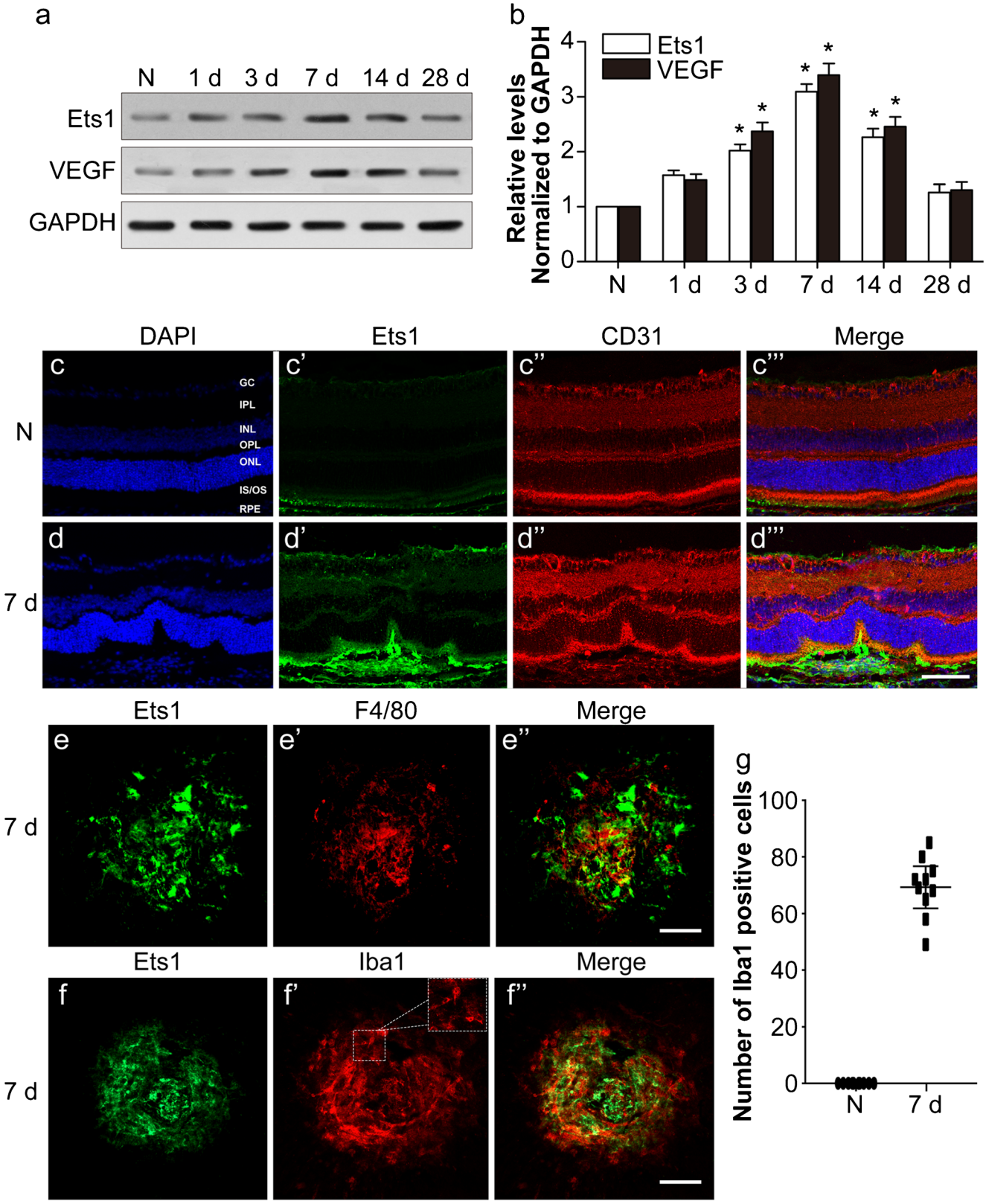

Ets1 expression following Ets1 siRNA treatment and laser injury was measured, showing that the Ets1 protein level in RPE-choroid-retina complexes reduced dramatically in Ets1 siRNA and ranibizumab (RBZ) groups compared with that in the CNV 7-day, vehicle and scramble siRNA groups (Fig. 2a, b).

◀ **Fig. 1** Ets1 increases and localizes in the CNV region. The mouse laser-induced CNV model was performed. (a) Western blot and (b) quantification analysis of Ets1 and VEGF expression in mouse choroid-RPE-retina complex took GAPDH as the loading control. $^{*}P < 0.05$ vs each normal group. (c, c', c", c"', d, d', d", d"') Choroid-RPE-retina tissues were sectioned and stained with the nuclear marker DAPI (blue), anti-Ets1 (green) and anti-CD31 (a vascular endothelial marker, red) antibodies. Scale bar = 50 μm. $n = 3$ in each group. (e, e', e") At day 7 after laser injury, mouse choroidal flat mounts were stained with anti-Ets-1 (green) and anti-F4/80 (red) antibodies. (f, f', f") At day 7 after laser injury, mouse choroidal flat mounts were stained with anti-Ets-1 (green) and anti-Iba1 (red) antibodies. Scale bar = 100 μm. $n = 3$ in each group. (g) Quantification of Iba1-positive cells in normal and CNV 7-day groups

Fundus fluorescein angiography (FFA) (Fig. 2c"", c""') and indocyanine green angiography (ICGA) (Fig. 2d"", d""') showed that the leakage area of CNV decreased in the Ets1 siRNA and RBZ groups. The data suggest that Ets1 inhibition ameliorates the leakage of CNV.

Ets1 siRNA inhibits laser-induced neovascularization and the dysfunction of RPE cells

The main source of FAF is lipofuscin granules (LGs), which accumulate in RPE cells (Schmitz-Valckenberg et al. 2008). LGs are formed by the incomplete lysosomal degradation of outer-segment photoreceptor cell debris resulting from the phagocytosis of RPE cells (Guha et al. 2014). FAF suggested that following laser treatment, LGs accumulated in the injury site, while Ets1 siRNA or RBZ downregulated the aggregation of LGs (Fig. 3a", a"', e).

The normal morphology of the choroid-RPE complex was visualized in non-lasered mouse eyes by confocal microscopy. Phalloidin (an F-actin-specific marker)-label identified the actin bundles of RPE cells forming a tightly packed, uniform hexagonal monolayer (Fig. 3b). No IB4 (a vasculature endothelial cell marker)-labeled endothelial cells were visualized in

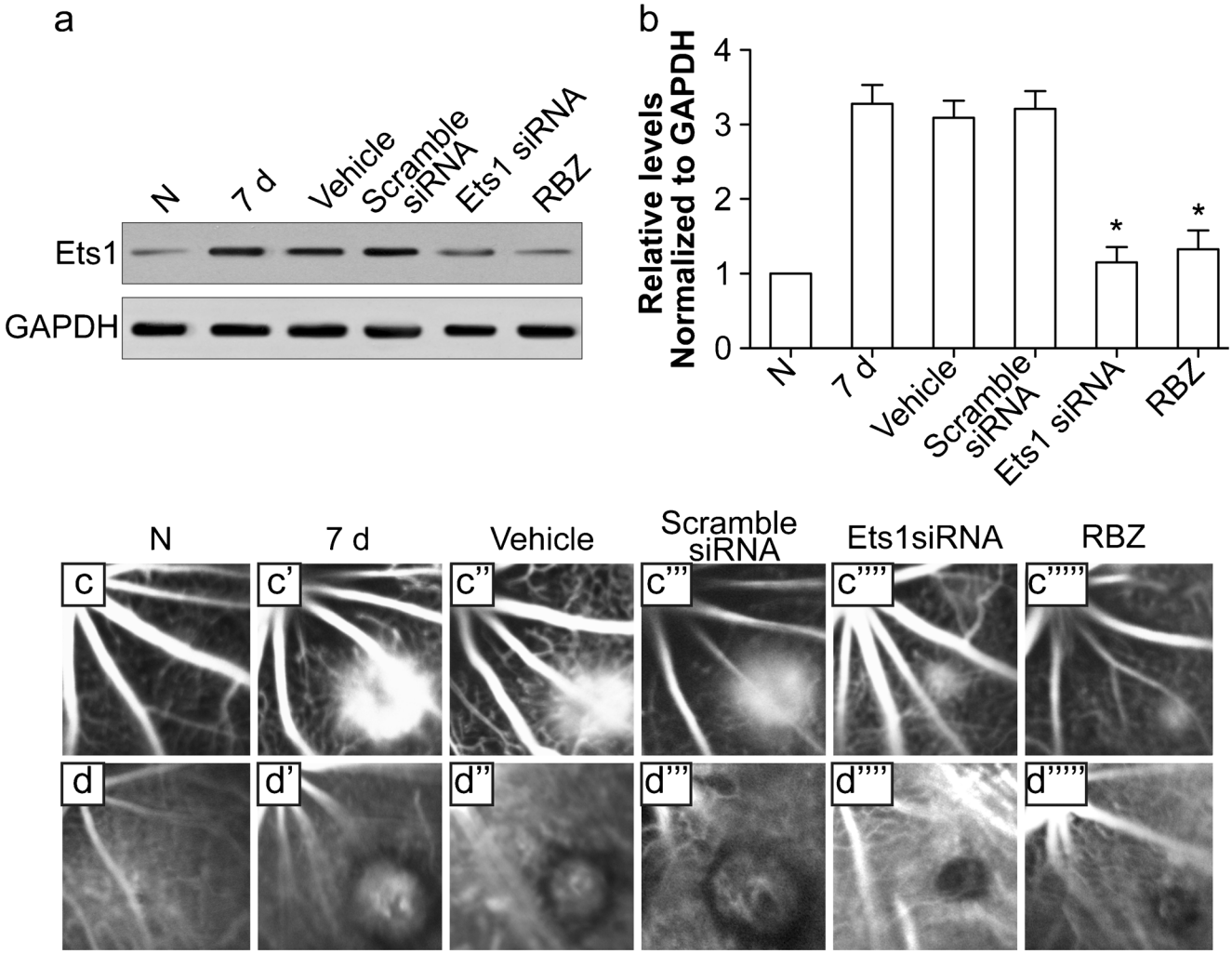

Fig. 2 Ets1 siRNA ameliorates the accumulation of RPE cells and the leakage of CNV. Mice were randomly divided into normal, CNV 7-day, CNV 7-day plus vehicle (PBS), CNV 7-day plus scramble siRNA, CNV 7-day plus Ets1 siRNA and CNV 7-day plus ranibizumab (RBZ) groups. (a) Western blot and (b) quantification analysis of Ets1 expression in mouse choroid-RPE-retina complex were performed in each group. $^{*}P < 0.05$ vs CNV 7-day group. (c, c', c", c"', c"", c""') Fundus fluorescein angiography (FFA) and (d, d', d", d"', d"", d""') indocyanine green angiography (ICGA) were performed in each group. $n = 3$ in each group

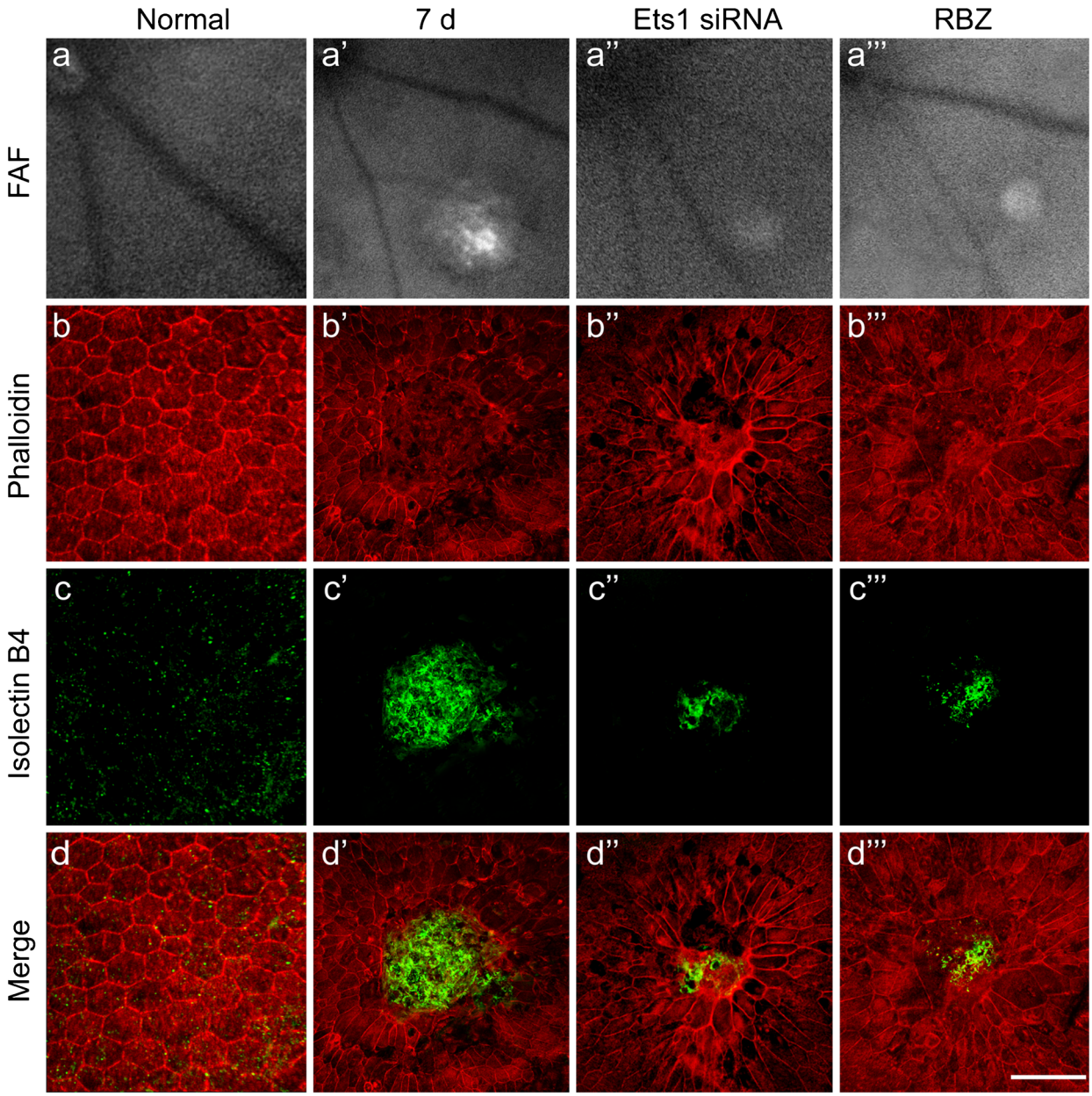
Normal
7 d
Ets1 siRNA
RBZ
FAF
Phalloidin
Isolectin B4
Merge
a
a'
a''
a'''
b
b'
b''
b'''
c
c'
c''
c'''
d
d'
d''
d'''

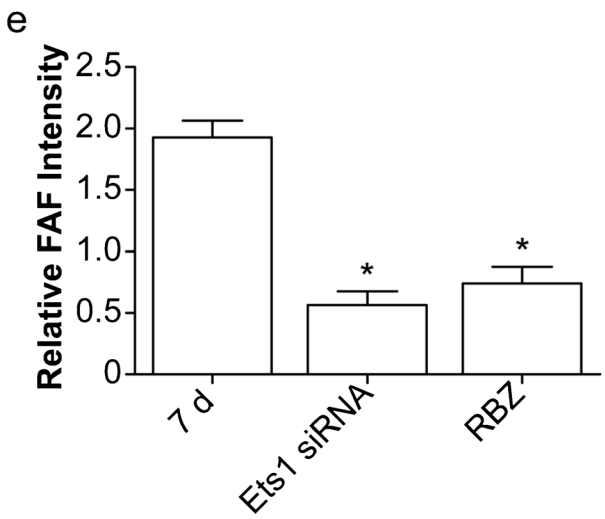
e
Relative FAF Intensity
2.5
2.0
1.5
1.0
0.5
0
*
*
7 d
Ets1 siRNA
RBZ

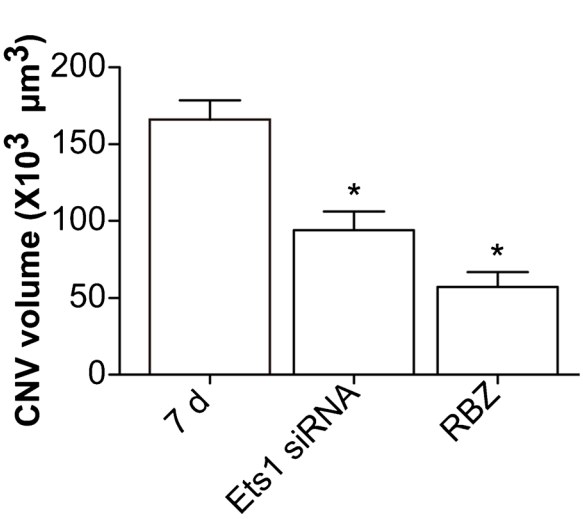
f
CNV volume (X10³ µm³)
200
150
100
50
0
*
*
7 d
Ets1 siRNA
RBZ

◀ **Fig. 3** Ets1 siRNA inhibits laser-induced neovascularization and RPE cell dysfunction. Mouse choroid flat mounts were from normal, CNV 7-day, CNV 7-day plus Ets1 siRNA and CNV 7-day plus RBZ groups. (a, a', a", a"') Fundus autofluorescence (FAF) was performed in each group. $n = 3$ in each group. (b, b', b", b"', c, c', c", c"', d, d', d", d"') Mouse choroid flat mounts from normal, CNV 7-day, CNV 7-day plus Ets1 siRNA and CNV 7-day plus RBZ groups were stained with phalloidin that represented RPE cells (red) and IB4 (green). Scale bar = 100 μm. $n = 3$ in each group. (e) Quantification analysis of relative FAF density. $^*P < 0.05$ vs CNV 7-day group. (f) Quantification analysis of CNV volume. $^*P < 0.05$ vs CNV 7-day group

the RPE layer (Fig. 3c, d). By 7 days, a well-defined radial array of IB4-labeled vessels was visible in the lesion and phalloidin-labeled RPE cells covered the area of the CNV complex (Fig. 3b', c', d'). Ets1 siRNA IVT injection reduced IB4-labeled vessels and reversed the hexagonal morphology of RPE cells in the lesion (Fig. 3b", c", d"). The quantitative analyses showed that the CNV area was reduced by Ets1 siRNA or RBZ compared to the CNV 7-day group (Fig. 3f). The results indicate that Ets1 siRNA inhibits laser-induced neovascularization and RPE cell dysfunction.

Ets1 siRNA alleviates CNV and downregulates the activation of macrophages/microglia

Since Ets1 plays a pro-inflammatory role (Feng et al. 2012; Zhao et al. 2018), Ets1 and F4/80 double-stain of choroidal flat mount was performed, showing that Ets1 was expressed by macrophages and microglia in the CNV region (Fig. 4b"'). To further identify the role of Ets1 in macrophages and microglia during CNV, IB4 and CD68 (activated macrophage/microglia marker) double stain of choroidal flat mount was applied, displaying that Ets1 siRNA downregulated the activation of macrophages and microglia (Fig. 4e', e", g). Meanwhile, Ets1 siRNA reduced the CNV volume (Fig. 4e, f). The data suggest that Ets1 siRNA alleviates CNV probably via downregulating the activation of macrophages and microglia.

Discussion

Ets1 acts as a pro-angiogenic transcription factor in wound angiogenesis (Chan et al. 2012), multiple tumors such as bladder cancer (Hui et al. 2018) and gastric cancer (Li et al. 2015). Firstly, we found that the Ets1 expression increased in the mouse laser-induced CNV model, in line with the previous study finding that the Ets1 mRNA level increases in a laser-induced mouse CNV model (Kinoshita et al. 2014). The overexpression of miR-129 inhibits PC-3 cell (a human prostate cancer cell line) viability, proliferation, migration and invasion through targeting Ets1 by phosphatidylinositol 3-kinase (PI3K)/Akt/mammalian target of rapamycin (mTOR) signaling pathway (Xu et al. 2017). The activation of the PI3K/AKT/mTOR pathway contributes to the progression of CNV (Sasore et al. 2014). For example, accumulation of hypoxia-inducible factor 1α (HIF-1α), a central pro-angiogenic molecule in CNV (Andre et al. 2015; Peet et al. 2017), is upregulated by the PI3K/Akt/mTOR signaling pathway (Garcia-Maceira and Mateo 2009). Therefore, whether Ets1 expression is upregulated by the PI3K/Akt/mTOR signaling pathway during CNV needs further investigation.

RBZ (Lucentis; Genentech Inc.) is an anti-VEGF monoclonal antibody (Berg et al. 2015). The US Food and Drug Administration approved RBZ (Lucentis; Genentech Inc.) for ophthalmological use in June 2006. In this study, we used RBZ as a positive control, which also downregulated Ets1 expression (Fig. 2a, b), indicating that Ets1 is a downstream molecule of VEGF. These results are consistent with previous researches (Bhattacharya et al. 2018; Ghosh et al. 2012; Konno et al. 2004). Inversely, Ets1 has been shown to regulate the expression of the two VEGF receptors including VEGFR1 and VEGFR2 (Kappel et al. 1999; Wakiya et al. 1996). Therefore, target Ets1 can block the vicious circle and alleviate CNV.

RPE cells contribute to the progression of CNV. Neovascular AMD triggers the dysfunction of RPE cells and signaling pathways involving inflammation and angiogenesis in RPE cells (Cai et al. 2014). During CNV, RPE cells release monocyte chemotactic protein (MCP), a cytokine promoting macrophage recruitment (Grossniklaus et al. 2002). Additionally, RPE cells also produce VEGF to facilitate angiogenesis (Grossniklaus et al. 2002; Spilsbury et al. 2000; Wang et al. 2016). In our study, LGs aggregated in the mouse CNV region and the morphology of RPE cells changed compared to that of the normal group, while Ets1 siRNA IVT injection reversed the dysfunction of RPE cells (Fig. 3a–c), suggesting that Ets1 upregulates the dysfunction of RPE cells in the CNV region, playing the pro-angiogenic role.

There are two subtypes of macrophage including M1 and M2 (Mantovani et al. 2004). M1, also named pro-inflammatory macrophages, are considered to be important for the elimination of tumor cells and foreign organisms (Ma et al. 2010; Qin et al. 2012), whereas M2, or anti-inflammatory macrophages, are involved in angiogenesis, wound healing, chronic infection and tumorigenesis (Bility et al. 2016; He et al. 2017; Jetten et al. 2014; Zhou et al. 2015). Microglia, the third glial cell type of the retina, represents the tissue macrophage population of the central nervous system (Karlstetter et al. 2015). It has been revealed that the pathological shift of macrophage polarization may contribute to the pathogenesis of AMD. Human advanced AMD macula has a higher macrophage M1 to M2 chemokine transcript ratio compared to normal eye bank eyes (Cao et al. 2011). In a mouse CNV model, the expression of M1 macrophage markers and cytokines increase to a greater extent compared

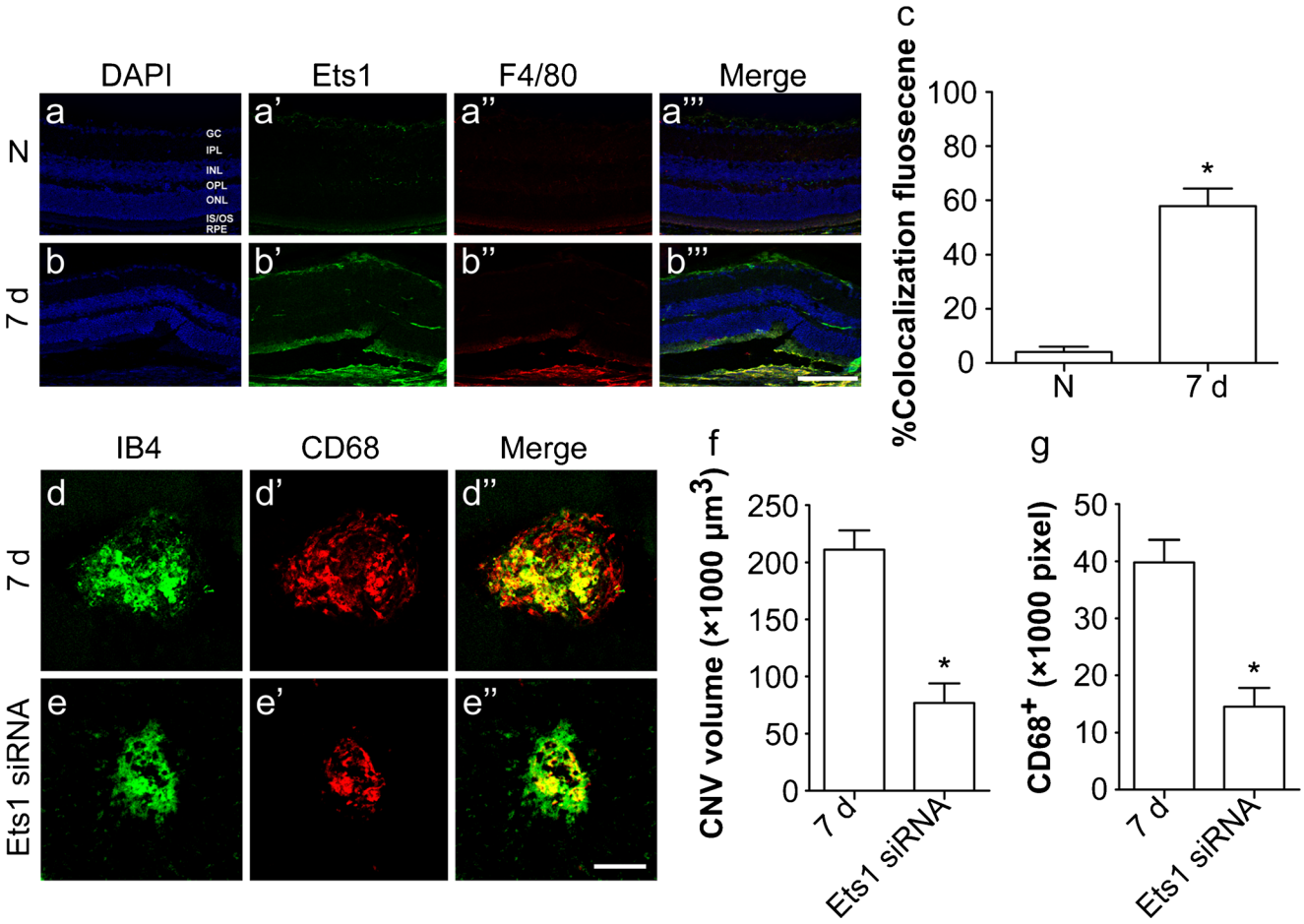

Fig. 4 Ets1 siRNA alleviates CNV and downregulates the activation of macrophages/microglia. The mice were randomly divided into normal and CNV 7-day groups. (a, a', a", a"', b, b', b", b"') Mouse choroid-RPE-retina tissues were sectioned and stained with anti-Ets-1 (green) antibody, anti-F4/80 (red) antibody and DAPI. (c) Fluorescence (integrated density) was measured in confocal photographs as those depicted in (a) using ImageJ Software. Co-localization fluorescence is referred to as concurrence points of green (Ets-1) and red (F4/80) fluorescence. (d, d', d", e, e', e") Mouse choroidal flat mounts were stained with anti-IB4 (green) and anti-CD68 (red) antibodies. Scale bar = 100 μm. $n = 3$ in each group. (f) Quantification analysis of CNV volume from mouse choroidal flat mount IB4 stain. *$P < 0.05$ vs CNV 7-day group. (g) Quantification analysis of CD68 positive cells from mouse choroidal flat mount CD68 stain. *$P < 0.05$ vs CNV 7-day group

with M2 markers in the RPE-choroid complexes following laser photocoagulation (Zhou et al. 2017). TNF-α deficiency downregulates the polarization of M1 macrophages, therefore attenuating experimental autoimmune neuritis (EAN) in mice (Zhang et al. 2012). TNF-α directly upregulates matrix metalloproteinase 9 (MMP9) and matrix metalloproteinase 2 (MMP2), which are linked to the activation of M1 macrophages (Ashcroft et al. 2012). These studies indicate that TNF-α promotes the polarization of M1 macrophages. Researchers have demonstrated a signal circuit from Ets1 to TNF-α as a single transcription factor (TF)-gene regulatory pathway step in human adipocytes induced from adipose tissue-derived stromal cells (Zhang et al. 2016). Moreover, TNF-α expression is upregulated by Ets1 (Kramer et al. 1995). Therefore, we suggest a hypothesis that Ets1 modulates macrophage/microglia polarization during CNV via promoting the transcription of TNF-α, which calls for future study.

Our data also showed that Ets1 was co-localized with Iba1 (a microglia marker) and increased following CNV in choroidal flat mount (Fig. 1e). However, Iba1 was not detected in the normal group (Fig. 1f), indicating barely any microglia in the choroid tissues under physiological condition, which is consistent with previous studies (Chen et al. 2014; Sheets et al. 2013). Microglia are the resident immune cells in the central nervous system (CNS) similar to macrophage type (Katsumoto et al. 2018). Changes in parenchymal microglia, including increased major histocompatibility complex class II (MHC-II) expression and morphological changes suggestive of activation, are related to early AMD (Penfold et al. 1997). In advanced AMD, activated amoeboid microglia infiltrate the outer nuclear layer (ONL) and subretinal space of the degenerating outer retina, where they participate in neovascular structures (Combadiere et al. 2007) and play a role in the phagocytosis of photoreceptor debris (Gupta et al.

2003). However, the functional differences between microglia and macrophage in AMD pathogenesis need further investigation.

In conclusion, the study reveals a novel role and mechanism of Ets1 in modulating CNV progression, in which the downregulation of Ets1 ameliorates CNV through inhibiting the dysfunction of RPE cells and the activation of macrophages/microglia. Thus, our study highlights the important role of Ets1 in CNV development and Ets1 is a potential therapeutic target for CNV treatment.

Funding information The study was supported by the Suzhou Science and Technology Bureau (No. SYS2018005), Suzhou Commission of Health and Family Planning (No. KJXW2018076), Jiangsu Distinguished Medical Experts Program (No.2016), Gusu Health Leading Talent Plan (Grant No. 025) and the 14th Six Talents Peak Project of Jiangsu Province (No. SWYY-058).

Compliance with ethical standards

Conflicts of interest The authors declare that they have no conflict of interest.

References

Andre H, Tunik S, Aronsson M, Kvanta A (2015) Hypoxia-inducible factor-1alpha is associated with sprouting angiogenesis in the murine laser-induced choroidal neovascularization model. Invest Ophthalmol Vis Sci 56:6591–6604

Ashcroft GS, Jeong MJ, Ashworth JJ, Hardman M, Jin W, Moutsopoulos N, Wild T, McCartney-Francis N, Sim D, McGrady G, Song XY, Wahl SM (2012) Tumor necrosis factor-alpha (TNF-alpha) is a therapeutic target for impaired cutaneous wound healing. Wound Repair Regen 20:38–49

Bakri SJ, Thorne JE, Ho AC, Ehlers JP, Schoenberger SD, Yeh S, Kim SJ (2019) Safety and efficacy of anti-vascular endothelial growth factor therapies for neovascular age-related macular degeneration: a report by the American Academy of Ophthalmology. Ophthalmology 126(1):55–63

Berg K, Pedersen TR, Sandvik L, Bragadottir R (2015) Comparison of ranibizumab and bevacizumab for neovascular age-related macular degeneration according to LUCAS treat-and-extend protocol. Ophthalmology 122:146–152

Bhattacharya R, Ray Chaudhuri S, Roy SS (2018) FGF9-induced ovarian cancer cell invasion involves VEGF-A/VEGFR2 augmentation by virtue of ETS1 upregulation and metabolic reprogramming. J Cell Biochem 119(10):8174–8189

Bility MT, Nio K, Li F, McGivern DR, Lemon SM, Feeney ER, Chung RT, Su L (2016) Chronic hepatitis C infection-induced liver fibrogenesis is associated with M2 macrophage activation. Sci Rep 6:39520

Cai Y, Li X, Wang YS, Shi YY, Ye Z, Yang GD, Dou GR, Hou HY, Yang N, Cao XR, Lu ZF (2014) Hyperglycemia promotes vasculogenesis in choroidal neovascularization in diabetic mice by stimulating VEGF and SDF-1 expression in retinal pigment epithelial cells. Exp Eye Res 123:87–96

Cao X, Shen D, Patel MM, Tuo J, Johnson TM, Olsen TW, Chan CC (2011) Macrophage polarization in the maculae of age-related macular degeneration: a pilot study. Pathol Int 61:528–535

Chan YC, Roy S, Huang Y, Khanna S, Sen CK (2012) The microRNA miR-199a-5p down-regulation switches on wound angiogenesis by derepressing the v-ets erythroblastosis virus E26 oncogene homolog 1-matrix metalloproteinase-1 pathway. J Biol Chem 287:41032–41043

Chen M, Glenn JV, Dasari S, McVicar C, Ward M, Colhoun L, Quinn M, Bierhaus A, Xu H, Stitt AW (2014) RAGE regulates immune cell infiltration and angiogenesis in choroidal neovascularization. PLoS One 9:e89548

Combadiere C, Feumi C, Raoul W, Keller N, Rodero M, Pezard A, Lavalette S, Houssier M, Jonet L, Picard E, Debre P, Sirinyan M, Deterre P, Ferroukhi T, Cohen SY, Chauvaud D, Jeanny JC, Chemtob S, Behar-Cohen F, Sennlaub F (2007) CX3CR1-dependent subretinal microglia cell accumulation is associated with cardinal features of age-related macular degeneration. J Clin Invest 117:2920–2928

D'Amore PA (1994) Mechanisms of retinal and choroidal neovascularization. Invest Ophthalmol Vis Sci 35:3974–3979

Feng W, Xing D, Hua P, Zhang Y, Chen YF, Oparil S, Jaimes EA (2010) The transcription factor ETS-1 mediates proinflammatory responses and neointima formation in carotid artery endoluminal vascular injury. Hypertension 55:1381–1388

Feng W, Chumley P, Hua P, Rezonzew G, Jaimes D, Duckworth MW, Xing D, Jaimes EA (2012) Role of the transcription factor erythroblastosis virus E26 oncogen homolog-1 (ETS-1) as mediator of the renal proinflammatory and profibrotic effects of angiotensin II. Hypertension 60:1226–1233

Feng W, Chumley P, Prieto MC, Miyada K, Seth DM, Fatima H, Hua P, Rezonzew G, Sanders PW, Jaimes EA (2015) Transcription factor avian erythroblastosis virus E26 oncogen homolog-1 is a novel mediator of renal injury in salt-sensitive hypertension. Hypertension 65:813–820

Ford KM, Saint-Geniez M, Walshe T, Zahr A, D'Amore PA (2011) Expression and role of VEGF in the adult retinal pigment epithelium. Invest Ophthalmol Vis Sci 52:9478–9487

Garcia-Maceira P, Mateo J (2009) Silibinin inhibits hypoxia-inducible factor-1alpha and Ranibizumab RBZ /p70S6K/4E-BP1 signalling pathway in human cervical and hepatoma cancer cells: implications for anticancer therapy. Oncogene 28:313–324

Ghosh S, Basu M, Roy SS (2012) ETS-1 protein regulates vascular endothelial growth factor-induced matrix metalloproteinase-9 and matrix metalloproteinase-13 expression in human ovarian carcinoma cell line SKOV-3. J Biol Chem 287:15001–15015

Grossniklaus HE, Ling JX, Wallace TM, Dithmar S, Lawson DH, Cohen C, Elner VM, Elner SG, Sternberg P Jr (2002) Macrophage and retinal pigment epithelium expression of angiogenic cytokines in choroidal neovascularization. Mol Vis 8:119–126

Guha S, Liu J, Baltazar G, Laties AM, Mitchell CH (2014) Rescue of compromised lysosomes enhances degradation of photoreceptor outer segments and reduces lipofuscin-like autofluorescence in retinal pigmented epithelial cells. Adv Exp Med Biol 801:105–111

Gupta N, Brown KE, Milam AH (2003) Activated microglia in human retinitis pigmentosa, late-onset retinal degeneration, and age-related macular degeneration. Exp Eye Res 76:463–471

Hashiya N, Jo N, Aoki M, Matsumoto K, Nakamura T, Sato Y, Ogata N, Ogihara T, Kaneda Y, Morishita R (2004) In vivo evidence of angiogenesis induced by transcription factor Ets-1: Ets-1 is located upstream of angiogenesis cascade. Circulation 109:3035–3041

He R, Yin H, Yuan B, Liu T, Luo L, Huang P, Dai L, Zeng K (2017) IL-33 improves wound healing through enhanced M2 macrophage polarization in diabetic mice. Mol Immunol 90:42–49

Heier JS, Brown DM, Chong V, Korobelnik JF, Kaiser PK, Nguyen QD, Kirchhof B, Ho A, Ogura Y, Yancopoulos GD, Stahl N, Vitti R,

Berliner AJ, Soo Y, Anderesi M, Groetzbach G, Sommerauer B, Sandbrink R, Simader C, Schmidt-Erfurth U, View, Groups VS (2012) Intravitreal aflibercept (VEGF trap-eye) in wet age-related macular degeneration. Ophthalmology 119:2537–2548

Huang H, Parlier R, Shen JK, Lutty GA, Vinores SA (2013) VEGF receptor blockade markedly reduces retinal microglia/macrophage infiltration into laser-induced CNV. PLoS One 8:e71808

Hui K, Wu S, Yue Y, Gu Y, Guan B, Wang X, Hsieh JT, Chang LS, He D, Wu K (2018) RASAL2 inhibits tumor angiogenesis via p-AKT/ETS1 signaling in bladder cancer. Cell Signal 48:38–44

Hussain RM, Ciulla TA (2017) Emerging vascular endothelial growth factor antagonists to treat neovascular age-related macular degeneration. Expert Opin Emerg Drugs 22:235–246

Jetten N, Verbruggen S, Gijbels MJ, Post MJ, De Winther MP, Donners MM (2014) Anti-inflammatory M2, but not pro-inflammatory M1 macrophages promote angiogenesis in vivo. Angiogenesis 17:109–118

Kaarniranta K, Sinha D, Blasiak J, Kauppinen A, Vereb Z, Salminen A, Boulton ME, Petrovski G (2013) Autophagy and heterophagy dysregulation leads to retinal pigment epithelium dysfunction and development of age-related macular degeneration. Autophagy 9:973–984

Kappel A, Ronicke V, Damert A, Flamme I, Risau W, Breier G (1999) Identification of vascular endothelial growth factor (VEGF) receptor-2 (Flk-1) promoter/enhancer sequences sufficient for angioblast and endothelial cell-specific transcription in transgenic mice. Blood 93:4284–4292

Karlstetter M, Scholz R, Rutar M, Wong WT, Provis JM, Langmann T (2015) Retinal microglia: just bystander or target for therapy? Prog Retin Eye Res 45:30–57

Katsumoto A, Takeuchi H, Takahashi K, Tanaka F (2018) Microglia in Alzheimer's disease: risk factors and inflammation. Front Neurol 9:978

Kinoshita S, Noda K, Tagawa Y, Inafuku S, Dong Y, Fukuhara J, Dong Z, Ando R, Kanda A, Ishida S (2014) Genistein attenuates choroidal neovascularization. J Nutr Biochem 25:1177–1182

Konno S, Iizuka M, Yukawa M, Sasaki K, Sato A, Horie Y, Nanjo H, Fukushima T, Watanabe S (2004) Altered expression of angiogenic factors in the VEGF-Ets-1 cascades in inflammatory bowel disease. J Gastroenterol 39:931–939

Kramer B, Wiegmann K, Kronke M (1995) Regulation of the human TNF promoter by the transcription factor Ets. J Biol Chem 270:6577–6583

Li Z, Liu Z, Dong S, Zhang J, Tan J, Wang Y, Ge C, Li R, Xue Y, Li M, Wang W, Xiang X, Yang J, Ding H, Geng T, Yao K, Song X (2015) miR-506 inhibits epithelial-to-mesenchymal transition and angiogenesis in gastric Cancer. Am J Pathol 185:2412–2420

Li L, Heiduschka P, Alex AF, Niekamper D, Eter N (2017) Behaviour of CD11b-positive cells in an animal model of laser-induced choroidal neovascularisation. Ophthalmologica 237:29–41

Luckoff A, Caramoy A, Scholz R, Prinz M, Kalinke U, Langmann T (2016) Interferon-beta signaling in retinal mononuclear phagocytes attenuates pathological neovascularization. EMBO Mol Med 8:670–678

Luu J, Palczewski K (2018) Human aging and disease: lessons from age-related macular degeneration. Proc Natl Acad Sci U S A 115:2866–2872

Ma J, Liu L, Che G, Yu N, Dai F, You Z (2010) The M1 form of tumor-associated macrophages in non-small cell lung cancer is positively associated with survival time. BMC Cancer 10:112

Mantovani A, Sica A, Sozzani S, Allavena P, Vecchi A, Locati M (2004) The chemokine system in diverse forms of macrophage activation and polarization. Trends Immunol 25:677–686

Mettu PS, Wielgus AR, Ong SS, Cousins SW (2012) Retinal pigment epithelium response to oxidant injury in the pathogenesis of early age-related macular degeneration. Mol Asp Med 33:376–398

Oda N, Abe M, Sato Y (1999) ETS-1 converts endothelial cells to the angiogenic phenotype by inducing the expression of matrix metalloproteinases and integrin beta3. J Cell Physiol 178:121–132

Peet DJ, Kittipassorn T, Wood JP, Chidlow G, Casson RJ (2017) HIF signalling: the eyes have it. Exp Cell Res 356:136–140

Penfold PL, Liew SC, Madigan MC, Provis JM (1997) Modulation of major histocompatibility complex class II expression in retinas with age-related macular degeneration. Invest Ophthalmol Vis Sci 38:2125–2133

Qin H, Holdbrooks AT, Liu Y, Reynolds SL, Yanagisawa LL, Benveniste EN (2012) SOCS3 deficiency promotes M1 macrophage polarization and inflammation. J Immunol 189:3439–3448

Rofagha S, Bhisitkul RB, Boyer DS, Sadda SR, Zhang K, Group S-US (2013) Seven-year outcomes in ranibizumab-treated patients in ANCHOR, MARINA, and HORIZON: a multicenter cohort study (SEVEN-UP). Ophthalmology 120:2292–2299

Sasore T, Reynolds AL, Kennedy BN (2014) Targeting the PI3K/Akt/mTOR pathway in ocular neovascularization. Adv Exp Med Biol 801:805–811

Schmitz-Valckenberg S, Holz FG, Bird AC, Spaide RF (2008) Fundus autofluorescence imaging: review and perspectives. Retina 28:385–409

Schutt F, Bergmann M, Holz FG, Kopitz J (2002) Isolation of intact lysosomes from human RPE cells and effects of A2-E on the integrity of the lysosomal and other cellular membranes. Graefes Arch Clin Exp Ophthalmol 240:983–988

Sheets KG, Jun B, Zhou Y, Zhu M, Petasis NA, Gordon WC, Bazan NG (2013) Microglial ramification and redistribution concomitant with the attenuation of choroidal neovascularization by neuroprotectin D1. Mol Vis 19:1747–1759

Spilsbury K, Garrett KL, Shen WY, Constable IJ, Rakoczy PE (2000) Overexpression of vascular endothelial growth factor (VEGF) in the retinal pigment epithelium leads to the development of choroidal neovascularization. Am J Pathol 157:135–144

Strauss O (2005) The retinal pigment epithelium in visual function. Physiol Rev 85:845–881

Tseng WA, Thein T, Kinnunen K, Lashkari K, Gregory MS, D'Amore PA, Ksander BR (2013) NLRP3 inflammasome activation in retinal pigment epithelial cells by lysosomal destabilization: implications for age-related macular degeneration. Invest Ophthalmol Vis Sci 54:110–120

Wakiya K, Begue A, Stehelin D, Shibuya M (1996) A cAMP response element and an Ets motif are involved in the transcriptional regulation of flt-1 tyrosine kinase (vascular endothelial growth factor receptor 1) gene. J Biol Chem 271:30823–30828

Wang H, Han X, Wittchen ES, Hartnett ME (2016) TNF-alpha mediates choroidal neovascularization by upregulating VEGF expression in RPE through ROS-dependent beta-catenin activation. Mol Vis 22:116–128

Wei G, Srinivasan R, Cantemir-Stone CZ, Sharma SM, Santhanam R, Weinstein M, Muthusamy N, Man AK, Oshima RG, Leone G, Ostrowski MC (2009) Ets1 and Ets2 are required for endothelial cell survival during embryonic angiogenesis. Blood 114:1123–1130

Xu S, Ge J, Zhang Z, Zhou W (2017) MiR-129 inhibits cell proliferation and metastasis by targeting ETS1 via PI3K/AKT/mTOR pathway in prostate cancer. Biomed Pharmacother 96:634–641

Zhang HL, Hassan MY, Zheng XY, Azimullah S, Quezada HC, Amir N, Elwasila M, Mix E, Adem A, Zhu J (2012) Attenuated EAN in TNF-alpha deficient mice is associated with an altered balance of M1/M2 macrophages. PLoS One 7:e38157

Zhang XM, Guo L, Huang X, Li QM, Chi MH (2016) 4-Hydroxynonenal regulates TNF-alpha gene transcription indirectly via ETS1 and microRNA-29b in human adipocytes induced from adipose tissue-derived stromal cells. Anat Rec (Hoboken) 299:1145–1152

Zhao N, Zou H, Qin J, Fan C, Liu Y, Wang S, Shan Z, Teng W, Li Y (2018) MicroRNA-326 contributes to autoimmune thyroiditis by targeting the Ets-1 protein. Endocrine 59:120–129

Zhou W, Ke SQ, Huang Z, Flavahan W, Fang X, Paul J, Wu L, Sloan AE, McLendon RE, Li X, Rich JN, Bao S (2015) Periostin secreted by glioblastoma stem cells recruits M2 tumour-associated macrophages and promotes malignant growth. Nat Cell Biol 17:170–182

Zhou Y, Yoshida S, Kubo Y, Yoshimura T, Kobayashi Y, Nakama T, Yamaguchi M, Ishikawa K, Oshima Y, Ishibashi T (2017) Different distributions of M1 and M2 macrophages in a mouse model of laser-induced choroidal neovascularization. Mol Med Rep 15:3949–3956